Bulletin of the Seismological Society of America, Vol. 68, No. 2, pp. 369–382, April, 1978

FINE STRUCTURE OF AN OCEANIC CRUSTAL SECTION NEAR THE EAST PACIFIC RISE

BY D. V. HELMBERGER AND G. ENGEN

ABSTRACT

In this study we model synthetically a complete seismic profile of roughly 20-m.y.-old crust located to the west of the East Pacific Rise, 3.37S, 114.13W. The results indicate a rather strong velocity gradient below the sediments with little evidence of layering in the upper crust and a slightly dipping oceanic layer. The crust-to-mantle transition zone appears sharp providing a relatively good wave guide for multiple Moho reflections which are modeled synthetically to further test the usefulness of a layered earth model in explaining entire seismograms. The mantle head waves decay abruptly near 50 km which can be explained by the onset of a low-velocity zone in the upper mantle at about a depth of 12 km below the ocean surface.

INTRODUCTION

Recent studies suggest that the crust contains a substantial low-velocity zone (LVZ) near the crest of the East Pacific Rise which disappears as the crust ages [see Orcutt *et al.* (1976)]. There is also evidence that the oceanic crust thickens with age, Shor *et al.* (1970) and others. Woollard (1975) suggests this growth occurs at the base of the crust and is essentially transformed mantle material. The seismic parameters describing this basal layer are not well established, with Sutton *et al.* (1971) arguing for the existence of a high-velocity zone (HVZ) while Lewis and Snydsman (1976) suggest the development of a LVZ increasing with age. Most of these conclusions are based on prominent second arrivals which are apparent in many seismic profiles.

To clarify the effects of basal HVZ and LVZ, we took the Raitt (1963) standard oceanic model modifying it so as to preserve the first-arrival times. The model parameters are given in Table 1 with the synthetics shown in Figures 1, 2, and 3. These synthetics were generated by the application of the generalized ray theory (GRT) as discussed by Helmberger (1968) and used in previous oceanic modeling attempts [see Helmberger (1977) and Helmberger and Morris (1969)]. For simplicity, we included only those rays which penetrate the 6.7-km/sec layer describing the lower crustal and upper mantle response. The upper crustal response at these ranges is usually found to be quite simple in most observed profiles and can be modeled by a smooth velocity depth function as discussed in Helmberger (1977). Thus we can visualize a simple pulse arriving at nearly constant velocity on the heavy line indicated in the figures.

In the step responses of Figure 1 we can see the reflection from the top of the 7.5-km/sec layer followed by the reflection from the top of the mantle. The first four multiple reflections in the 7.5-layer were included in these calculations, although only two multiples were necessary for convergence to the same synthetics obtained for model A when the 7.5-layer is allowed to become very thin. The synthetics on the right are appropriate for a 20-pound charge fired with the standard shooting setup [see Helmberger (1968)]. The synthetics in the middle column were generated by compressing the time scale of the transfer function by two which allows the apparent velocities of 7.5 and 8.1 to be more easily recognized.

The apparent velocities between 6.7 and the mantle velocity of 8.2 are observed

on numerous air gun profiles at small ranges, 15 to 30 km, as reported by Maynard (1970) and Sutton *et al.* (1971). The short-period nature of these experiments makes it much easier to observe such details as can be seen in Figure 1. Unfortunately, air gun data is essentially processed mechanically and is usually not available to the synthetic modeling technique.

The LVZ case is displayed in Figure 2 where the most distinguishing feature is

TABLE 1
MODEL PARAMETERS

Thickness (km)	*P* Velocity (km/sec)	*S* Velocity (km/sec)	Density (gr/cm^3)
	A. (Raitt Oceanic Model)		
3.00	1.50	0.0	1.00
0.45	2.00	0.50	1.10
1.75	5.00	3.50	2.50
4.70	6.70	3.80	2.60
	8.10	4.60	3.40
	B. (HVZ Transition)		
4.50	1.50	0.0	1.00
0.45	2.00	0.50	1.10
1.75	5.00	3.50	2.50
4.10	6.70	3.80	2.60
1.00	7.50	4.26	3.06
	8.10	4.60	3.40
	C. (LVZ Transition)		
4.50	1.50	0.0	1.00
0.45	2.00	0.50	1.10
1.75	5.00	3.50	2.50
3.37	6.70	3.80	2.60
1.00	6.00	3.68	2.56
	8.10	4.60	3.40
	D. (Down-Dip)		
4.50	1.50	0.0	1.00
0.45	2.00	0.50	1.10
1.75	5.00	3.50	2.50
4.70	6.70	3.80	2.60
	8.38	4.72	3.52
	E. (Up-Dip)		
4.50	1.50	0.0	1.00
0.45	2.00	0.50	1.10
1.75	5.00	3.50	2.50
4.70	6.70	3.80	2.60
	7.86	4.47	3.26

the lateness of the Moho reflection. This feature is evident in many of the excellent profiles presented by Lewis and McClain (1977) and Lewis and Snydsman (1976). A small amount of dipping structure can also produce this effect. In Figure 3 we present results from models D and E where the oceanic layer has a 1.5° dip. The synthetics for model A are superimposed for comparison. For these small angles the transmission and reflection coefficients are essentially the same as in the flat case with the only significant change taking place in the travel times [see Hong and Helmberger (1977) for a general description of this problem]. If we examine the

standard synthetics it is clear that the exact arrival time of the later pulses is difficult if not impossible to pick. In reality these seismograms would be complicated more by the upper crustal arrival at 6.7 and wave shapes and relative amplitudes become important in deciding which of the above cases suits a given profile. Also, the delay times and apparent velocities could be direction dependent and the need for reversed profiles becomes obvious.

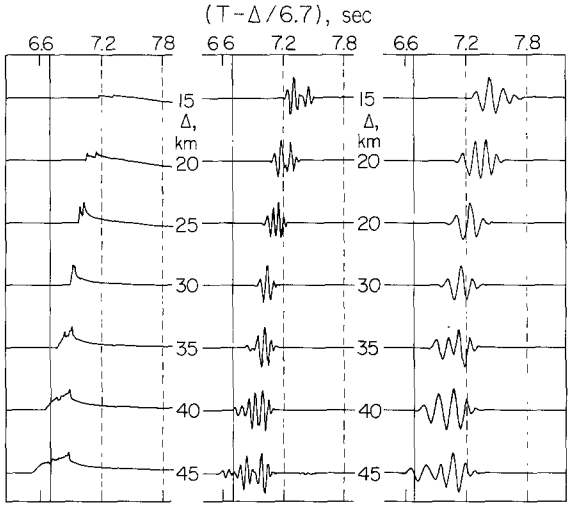

FIG. 1. Responses for the model B (HVZ transition) given in Table 1, plotted on a reduced travel-time section. The solid lines at times of 6.68 sec correspond to the crustal arrival times with the crossover occurring near 38 km.

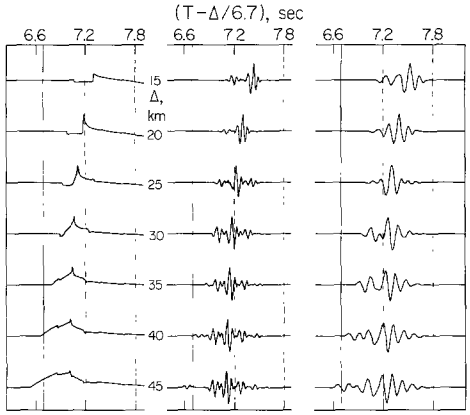

FIG. 2. Responses for the model C (LVZ transition) given in Table 1, plotted on a reduced travel-time section. The solid lines at time of 6.68 sec correspond to the crustal arrival times with the crossover occurring near 38 km.

After the above introduction it should be apparent that we need broadband data with multi-reversed profiles to understand a simple layered stack model adequately. However, in the absence of such idealized data we selected a seemingly well behaved profile for detailed analysis to further study crustal structure near a rise. The selection, DW37, was taken from the excellent data library at Scripps, and was chosen because of its location near the East Pacific Rise but far enough removed to avoid the rough topography near the rise crest. The location and orientation of this profile relative to the rise structure is given in Figure 4.

RESULTS

The record section studied here was taken on the Downwind expedition and was discussed by Shor *et al.* (1970) along with other profiles in this region of the Pacific. The recording set-up is described by Raitt (1956) and consists of three hydrophones recording a line of shots of varying charge sizes. This particular profile was shot in the usual split arrangement. The digitized traces from hydrophone three are displayed in Figures 5 and 6. The recordings near 10 km are not particularly useful because of the interference effects produced by the direct water wave crossing

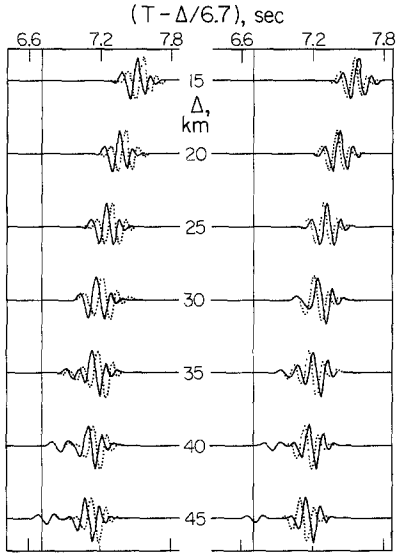

FIG. 3. Comparison of synthetics from model A with model D (down-dip) on the *left* and with model E (up-dip) on the *right.*

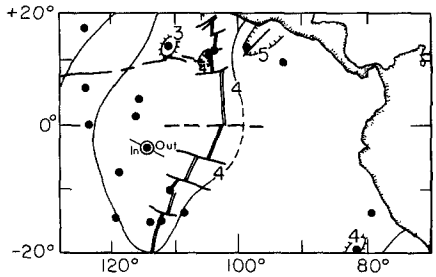

FIG. 4. Map of East Pacific Rise in the area of the split profile used in this study. DW37 location is indicated by dark circle with second circle surrounding it at 3.37°S, 114.13°W. Black dots are other profiles reported on by Shor *et al.* (1971).

through the head wave and are omitted from consideration. The recordings from the other end of the split profile are similar but are rather noisy because of stormy sea conditions. Included in Figures 5 and 6 are some synthetics, based on crustal model 1 displayed in Figure 7, which we will now consider at length.

The search strategy used in finding these models is the usual one; that is, we first obtain a layered model that fits the travel time followed by a comparison between observations and synthetics. Adjustments are then made by examining the strengths of various generalized rays until most of the important features are matched.

The details of the upper crustal model are determined by the match of the synthetics with observations displayed in Figure 5. The recordings are aligned with

respect to the bottom reflection which can be read accurately on the high-frequency channels designed for that purpose [see Raitt (1956)]. This timing is especially valuable at the beginning of profiles in that the charge size seems to be constantly

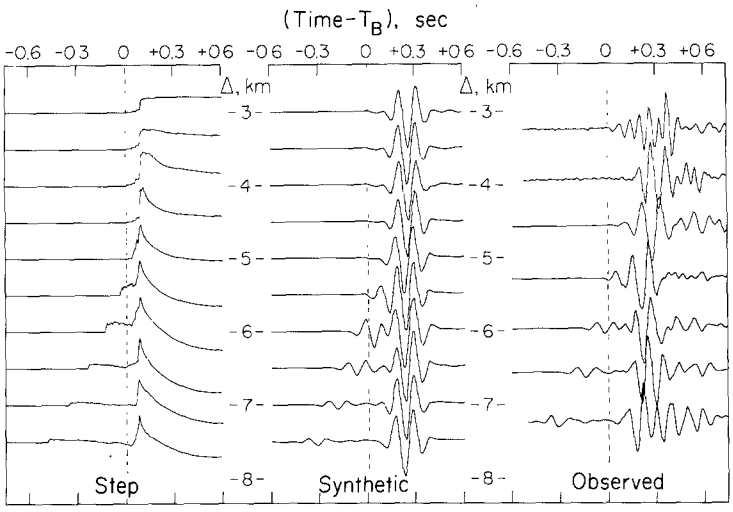

FIG. 5. Step responses and synthetics based on model 1 given in Figure 7 for a 2-pound shot compared with the observations of DW37 incoming.

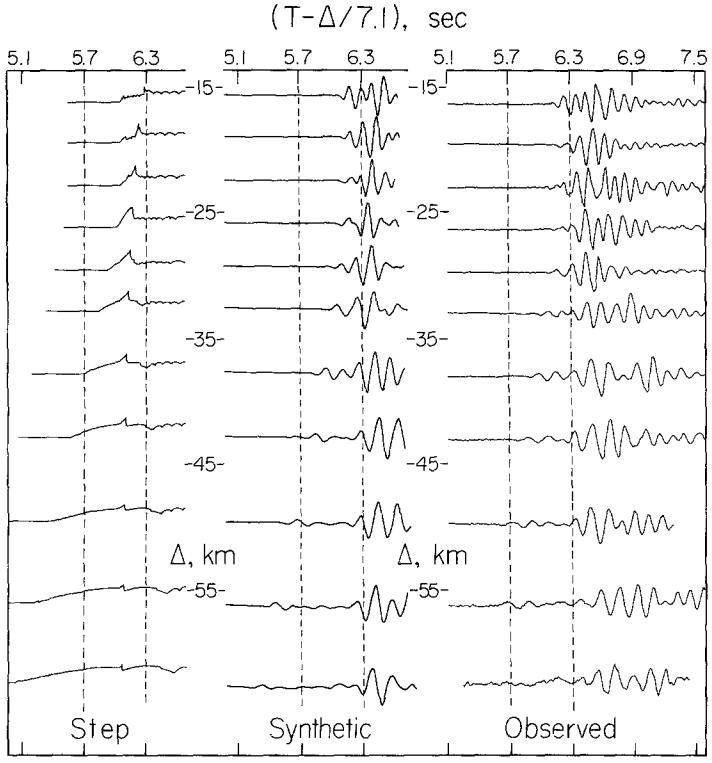

FIG. 6. Step responses and synthetics based on model 1 given in Figure 7 with a 1° dip in oceanic layer compared with observations of DW37 incoming.

changing at this stage of the shooting schedule. For instance the top three observations in Figure 5 are of three different charge sizes as can be surmised by the change in period. These changes in shot sizes and associated depths drastically alter

the source periodicity causing uncertainty in distinguishing which characteristics are model dependent and which are source dependent. The resulting changes in surface reflection times also make it difficult to align the traces. Thus, we concentrated our efforts on the sub-bottom structure and the development of the head wave. The match of the synthetics beyond 4 km is quite good and could probably be better if we had a more accurate source description. However, the overall amplitude ratios and timing are good, thereby providing a powerful constraint on the model as discussed by Spudich (1977) and others. Note that the step function response for the head wave is nearly a step which is the same situation found in the study by Helmberger and Morris (1969) and Helmberger (1977). This feature of synthetic modeling suggests a relatively strong velocity gradient in the upper crust without large distinct layering, a conclusion further documented by Orcutt *et al.* (1976), and Kennett and Orcutt (1976). On the other hand, it should be realized that small scale reflectors would not be recognized by these conventional refraction periods. There is, also, the problem of a gap in the record section near 10 km caused by the overload of the recording system by the powerful direct wave that intersects the head wave

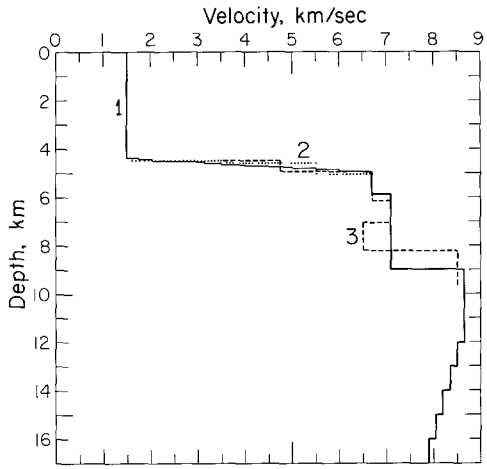

FIG. 7. Plots of velocity-depth functions used in the synthetics discussed in this report.

at this range. Thus, we continue the discussion of the model by switching our attention to Figure 6.

The strategy used in modeling this portion of the crustal section is essentially to assume that the first 0.2 sec of record at $\Delta = 16$ km is produced entirely by the upper crust and that the later portion is coming from the base of the crust. A similar interpretation was used in modeling a section in the Aleutian Basin (Helmberger, 1977), where one can see these two distinct pulses interact as they intersect in time. For example, the record at $\Delta = 16$ km would correspond to the record $\Delta = 38.4$ km in the LF13 section as displayed in Figure 8. The Aleutian Basin, being much older, has a considerably thicker crust; hence the disparity in distances. At larger ranges in Figure 6 we have three arrivals interacting; the crustal phase, the Moho refraction or mantle wave, followed by the Moho reflection. Therefore, we should not be surprised by the rapid changes in wave forms between 22 and 30 km. At still larger ranges, things become simple again with the mantle pulse separating from the slower crustal arrivals.

We can now use the experience gained from studying Figures 1, 2, and 3 to move the Moho response around in time as well as change its amplitude by adjusting critical angles. A relatively large number of models were considered in this trial and

error search but for brevity we will discuss only the three models given in Figure 7.

First, the synthetics given in Figure 6 were generated from model 1 using only the primary rays, thereby yielding a limited portion of record. A dip of 1° was applied to the oceanic layer (7.1 km/sec layer) for timing purposes. We applied a negative velocity gradient in the mantle to effectively eliminate the mantle head wave [see Helmberger and Morris (1969) and Hill (1971)]. Synthetics for a somewhat coarser layered model (2) are given in Figure 9 where the first set of multiples were included. In this case we did not apply the negative velocity gradient in the mantle for comparative purposes although we again applied a 1° dip to the oceanic layer. In Figure 10, we display synthetics based on model 3 which contains a LVZ but no dipping layers. We again included the first set of multiples although it should be

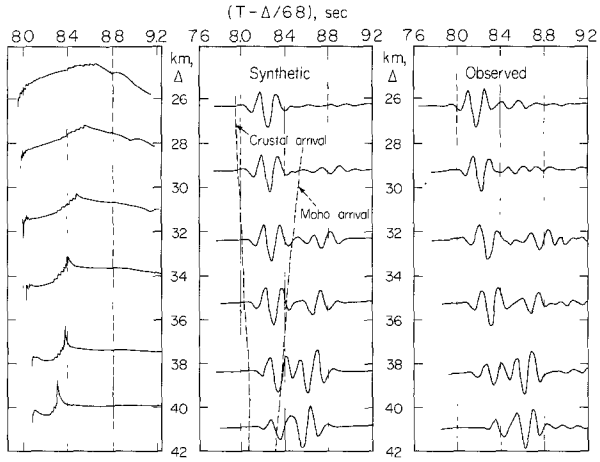

FIG. 8. Step responses and synthetics computed for Aleutian Basin compared with observations from LF13.

stressed that the tail of the synthetics at the largest range is probably inaccurate. That is, the inclusion of a LVZ in a model greatly increases the number of multiples required for convergence. However, second-order multiples were included in a synthetic run for the record at $\Delta = 50$ km with no noticeable change in character. The reflectivity method [Fuchs and Müller (1971)], has a distinct advantage in computing synthetics for this type of model. This method was used in the context of a model with a LVZ by Orcutt *et al.* (1976).

The addition of a LVZ to the model does effectively move the Moho reflection back as expected. However, as discussed earlier, a dipping layer can also accomplish this. Please note that whole individual records may have to be shifted in time up to 0.04 sec due to varying depths of the ocean which are not accounted for by the model. Therefore the most important considerations are the actual separation between the mantle head wave and Moho reflection and the relative amplitudes. We were unable to achieve a satisfactory relationship with the LVZ model. For example, it is clear in Figure 10 that the head wave is much too large out to 45 km. One can also see that the separation between the three phases is not good even at 15.9 km causing wave shapes that do not agree well with the observations. When we eliminated the low-velocity layer and applied the 1° dip to the 7.1 km/sec layer the separation and relative amplitudes, and, consequently, the overall fit, improved considerably. This can be seen quite well by overlay.

A more conventional method of detecting a dipping layer is by shooting reversed profiles and noting the shift in crossover distance and the asymmetry in the apparent velocities. A similar effect can be seen in this split profile as displayed in Figure 11.

The scatter in the travel-time data is severe, but it appears the crossover in the outgoing line occurs at a shorter distance which is compatible with the dipping

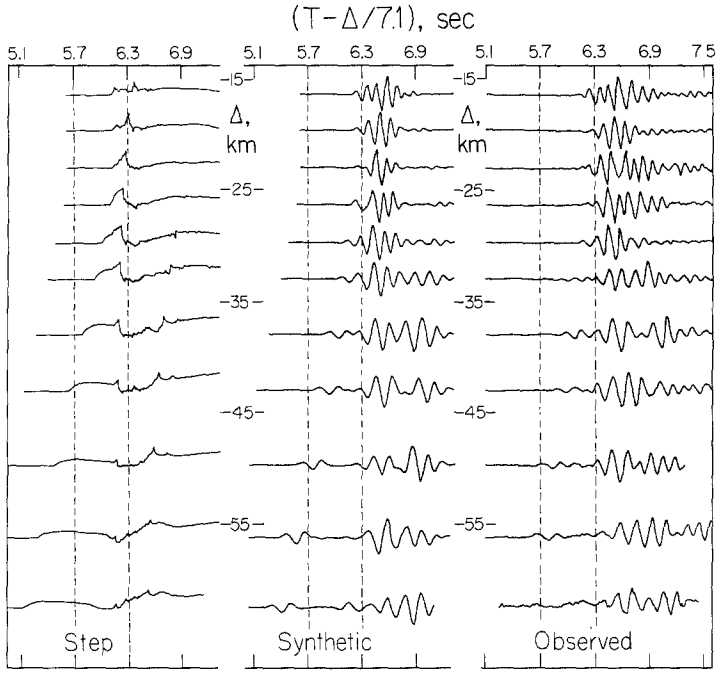

FIG. 9. Comparison of observations from DW37 with synthetics based on model 2 in Figure 7.

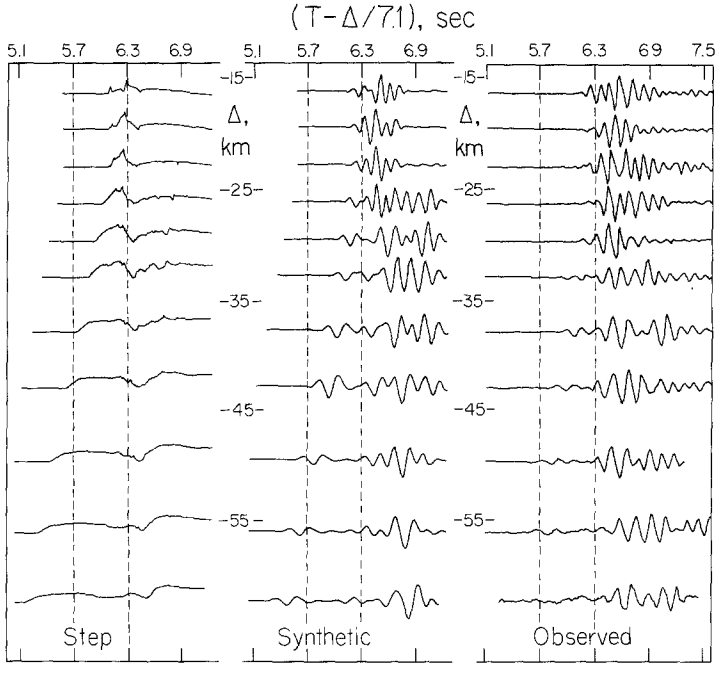

FIG. 10. Step responses and synthetics based on LVZ model 3 given in Figure 7 compared with observations of DW37 incoming.

model. The DW37 profile is oriented perpendicular to the isochrons (see Figure 4). Thus, although this effect could be a local phenomenon, both the travel times and wave forms are consistent with a crust that thickens with age.

We will next consider the remaining portions of the observations and see what can be explained by our model 2.

The DW37 record section is relatively simple in that there are not many unidentified signals as displayed in Figure 12. The large arrival which is off scale and moving slowly is the direct signal along a water path. Near 20 km a second arrival emerges which we will call PP. It occurs about 6 sec behind the first arrival and has crossed the water layer four times, thus the large delay. This pulse has been

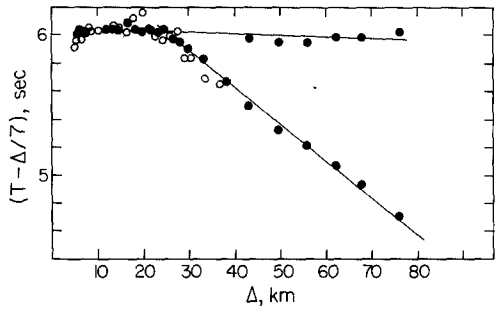

FIG. 11. Reduced travel times for DW37 with solid circles obtained from the incoming line and the open circles obtained from the outgoing line. Unfortunately, the first arrivals at the larger distances on the outgoing line are not apparent on the records because of background noise and the mantle velocity is difficult to estimate.

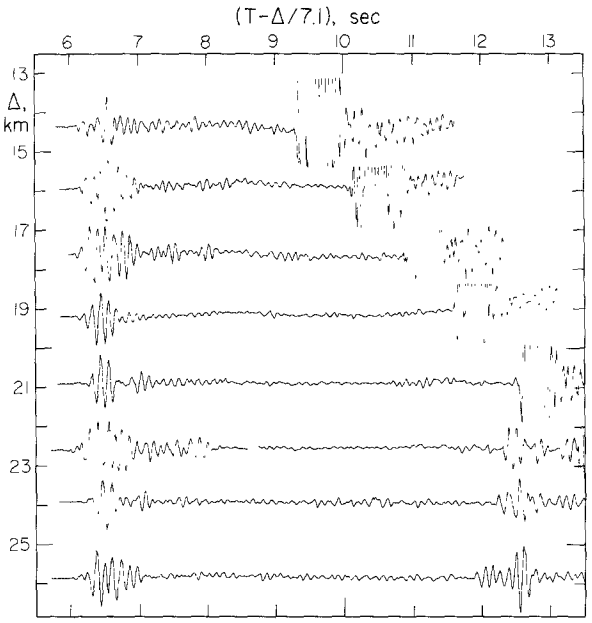

FIG. 12. Record section showing P, PP, and water wave.

discussed extensively in the literature [see Ewing (1963)] and is commonly observed. A reduced record section showing P and PP where the relative amplitude ratio is preserved is given in Figure 13. The erratic wave form pattern observed is typical with the PP usually stronger at the larger ranges. A similar pattern for PPP starts near 30 km with very little motion in the 6-sec gap.

The synthetic PP phase contains those rays that have crossed the water layer four times and have been reflected only twice from the various bottom interfaces (see Figure 14). These rays are the dominant contributions although higher order

multiples in the solid crust become important at the larger ranges. The Moho response is again the most powerful with its apparent 7.1 km/sec velocity. Note that the PP phase is controlled by nonsymmetric paths out to 30 km and is constructed by computing one ray description and doubling the response [see Hron and Kanasewich (1971) for this type of generalized ray redundancy]. Since the oceanic crust is not completely uniform we might expect these two paths in nature to be slightly different and thus produce some interference. The overall comparison of the observed PP phase and corresponding synthetics is not encouraging although the relative amplitudes are about right. Since the synthetics were generated assuming infinite Q we conclude that attenuation is not important at these frequencies.

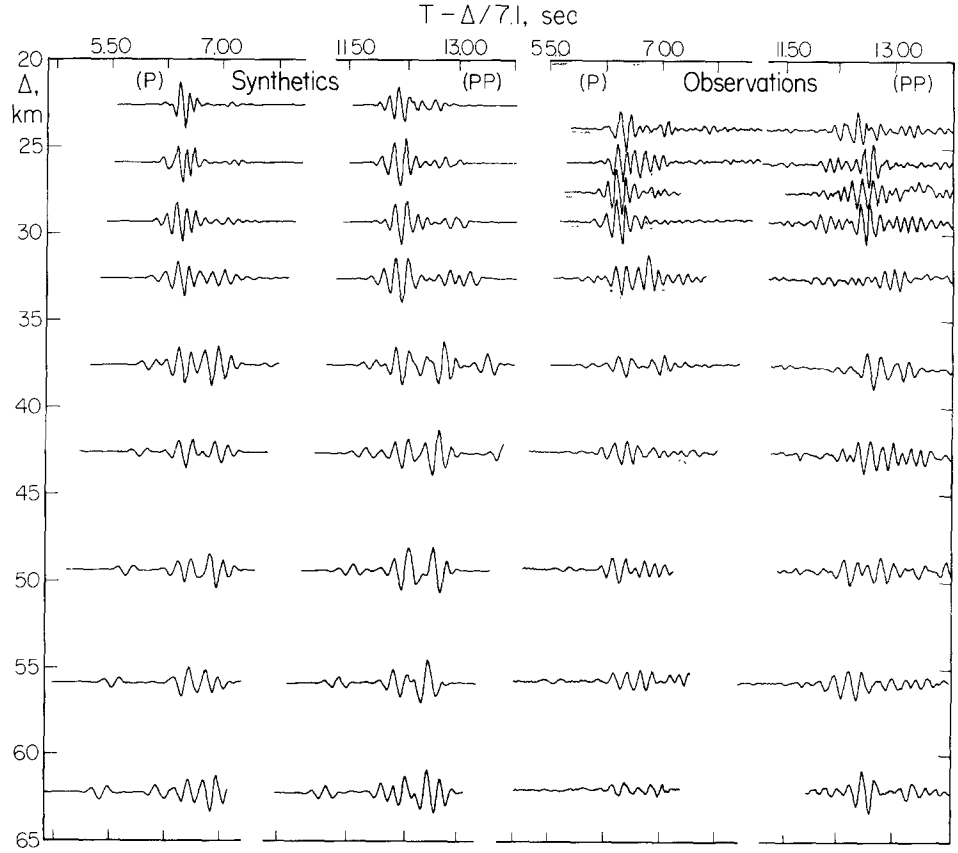

FIG. 13. Reduced section of synthetics and observations of P and PP.

DISCUSSION

The hydrophone data presented here is typical in many respects to hundreds of profiles taken in the Pacific which are described and discussed by Shor *et al.* (1970). Most of this data is difficult to examine in record section since it was recorded on paper; thus, the number of hand digitized record sections are few. However, there are some excellent record sections of hydrophone data that have recently been recorded on tape as discussed by Lewis and Snydsman (1976) and Lewis and McClain (1977). Some of these profiles are remarkably similar to DW37. On the other hand, most of the sections displaying OBS data are considerably different in character; for example, see the sections discussed by Orcutt *et al.* (1976). These record sections can be characterized by almost continuous signal starting with the

first arrival and growing in strength up to the direct water arrival and beyond. The problem is to understand the source of these signals which are not predicted nor accounted for by the model. Part of the complication could easily be scattered *PL* waves or converted shear waves as discussed by Lewis and McClain (1977) where they compare profiles of OBS and hydrophone data for the same shots. Another possibility is that OBS data has been taken in much more interesting locations than most hydrophone data, and clearly the section DW37 was not chosen for its complexity. Thus, the stability of the wave-form data must be investigated and the scale of the lateral variation examined. There is, also, the question of modeling philosophy in the presence of imperfect data.

The uniformity of the crustal arrival in the Aleutian Basin is remarkable [see Helmberger (1977)]. There are hundreds of crustal arrivals in the six or seven profiles in this old basin, probably older than 150 m.y., that are similar to the top trace of Figure 8. We think this could be due to the strong velocity gradient that

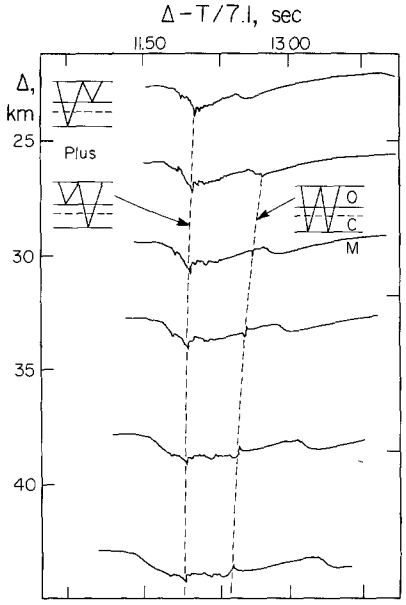

FIG. 14. Step responses of PP showing ray paths of dominant arrivals.

apparently develops in the aging oceanic crust, although we have not documented this effect by investigating other regions. On the other hand, the stability of the crustal arrival in DW37 is good but not excellent as can be seen in Figure 15.

As mentioned earlier we have three recordings for each shot which are at slightly different ranges. We selected the output for the two hydrophones with the greatest separation for this display and we have also included the synthetic for model 2 for comparison. We expect the stability of the observed wave forms to be the greatest at the smaller ranges before the Moho reflection reaches critical angle (see Figure 9). The situation is still somewhat complicated in that the Moho arrival does interfere with the crustal pulse as is quite evident in these comparisons. However, the beginning portion of the first three ranges should be primarily the crustal arrival which is not uniform even over a few hundred meters. This may mean that the velocity gradient in the upper oceanic layer is not as great in a younger crust as in the older situation, or perhaps the crust tends to eliminate small scale heterogeneity in the aging process. At larger ranges, near the crossover distance, the wave forms become quite complicated because of heavy interference as discussed earlier and

the development of multiple reflections inside the solid crust becomes important as indicated in Figure 9. The change in overall appearance of record sections at ranges beyond 35 km, postcrossover, is evident in Figure 15 as well as in the sections presented by Lewis and McClain (1977) and Lewis and Snydsman (1976). The correlation between the output of neighboring hydrophones is quite good through the Moho reflection and then begins to deteriorate. The same correlation holds between the synthetic and observed traces except that the synthetic head wave has not been attenuated by the low-velocity gradient in the mantle. The correlation between the synthetics and the observations that corresponds to internal multiples is distinctly bad. The situation could probably be helped by the addition of more layers to the model in that the internal reflection that produces this large pulse would be reduced. However, it is definitely not convenient to include more layers due to the expense in computing the synthetics using GRT. On the other hand, the

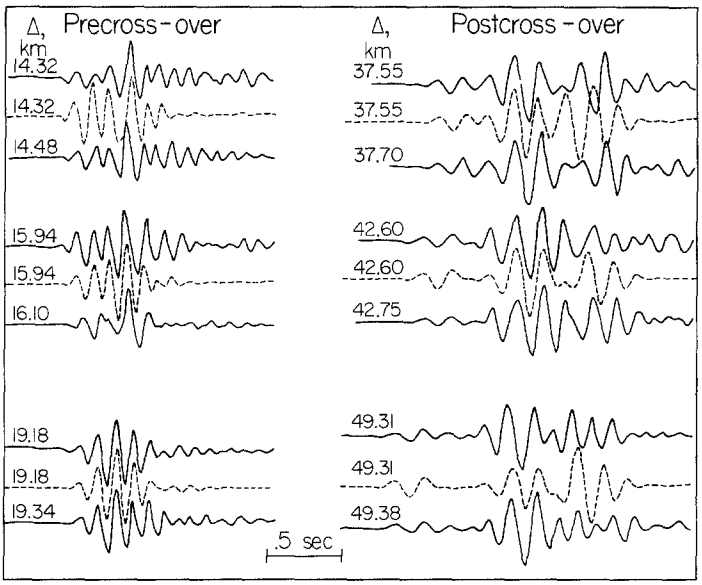

FIG. 15. Observations from 2 hydrophones (solid lines) with synthetic for model 2 (dotted lines) for comparison.

reflectivity method as introduced by Fuchs (1970) includes all reflections automatically and can be used to great advantage in this situation. But one must decide how important it is to model later arrivals. Do we attempt to fit the entire wave train treating each sample of record with equal importance or do we weight certain portions of records preferentially? We favor the latter approach since we think that the portions of the record that are dominated by primary arrivals such as the Moho reflection are observationally more stable than those portions dominated by multiples. This type of phenomenon was examined from a somewhat different point of view recently by Helmberger and Johnson (1977). This study involved modeling local earthquake records where the receiver structure was found to be very important in understanding the observed record. When the station is sitting on a soft layer, one can see arrivals that correspond to multiples in this layer which are easily modeled for the first few bounces. However, the ability to model the wave form for later times becomes increasingly difficult, which we interpret as a breakdown in the assumed flat layered model. One way to produce such an effect is to simply allow a small amount of dipping structure. Rays that pass directly through such a layer are

not affected whereas rays that are internally reflected a few times can be drastically altered; for example, see Hong and Helmberger (1977). The situation becomes even more interesting when the structure has dips and bumps which will be discussed at a later time. At any rate, this type of local scattering could be a real problem for OBS's as well as for extended wave trains involving multiples.

In conclusion, we have modeled a crustal section of 20-m.y.-old crust at about right angles to the rise crest and found an upper mantle velocity of 8.65 km/sec. This velocity was determined quite accurately and was unexpectedly high. Part of this velocity (0.3 km/sec) can be explained by anisotropy as discussed by Raitt *et al.* (1969). On the other hand, the velocity decreases rapidly with depth in that the head wave slows down and disappears beyond 60 km. The oceanic layer was found to be quite homogeneous with a sharp Moho which is considerably different from the much older crust found in the Aleutian Basin, probably over 150 m.y. old, with its strong velocity gradient and thicker oceanic layer overlying a 2 km crust-to-mantle transition. Thus, our results agree with those of Shor *et al.* (1970) and Sutton *et al.* (1971) on the thickening of the oceanic crust with age. These aging features could easily be accomplished by hydrothermal metamorphism as discussed by Woollard (1975), with the crustal thickening accounted for by a transformation of mantle material.

ACKNOWLEDGMENTS

We wish to express our thanks to George Shor and Russell Raitt of the Marine Physical Laboratory of the Scripps Institution of Oceanography for providing the data as well as for a number of useful discussions. This work was supported by the Office of Naval Research under Contract N00014-76-C-1070.

REFERENCES

Ewing, J. (1963). Elementary theory of seismic refraction and reflection measurements, in *The Sea,* **3,** 3–19, M. N. Hill, Editor, Interscience, New York.

Fuchs, K. (1960). On the determination of velocity depth distributions of elastic waves from dynamic characteristics of the reflected field, *Z. Geophys.* **36,** 531–548.

Fuchs, K. and Müller, G. (1971). Computation of synthetic seismograms with the reflectivity method and comparison with observations, *Geophys. J.* **23,** 417–433.

Helmberger, D. V. (1968). The crust-mantle transition in the Bering Sea, *Bull. Seism. Soc. Am.* **58,** 179–214.

Helmberger, D. V. (1977). Fine structure of an Aleutian crustal section, *Geophys. J.* **48,** 81–90.

Helmberger, D. V. and Johnson, L. R. (1977). Source parameters of moderate size earthquakes and the importance of receiver crustal structure in interpreting observations of local earthquakes, *Bull. Seism. Soc. Am.* **67,** 301–313.

Helmberger, D. V. and Morris, G. B. (1969). A travel time and amplitude interpretation of a marine refraction profile: Primary waves, *J. Geophys. Res.* **74,** 483–494.

Hill, D. P. (1971). Velocity gradients and anelasticity from crustal body wave amplitudes, *J. Geophys. Res.* **76,** 3309–3325.

Hong, T. L. and Helmberger, D. V. (1977). Generalized ray theory for dipping structure, *Bull. Seism. Soc. Am.* **67,** 995–1008.

Hron, F. and Kanasewich, E. R. (1971). Synthetic seismograms for deep seismic sounding studies using asymptotic ray theory, *Bull. Seism. Soc. Am.* **61,** 1169–1200.

Kennett, B. L. N. and Orcutt, J. A. (1976). A comparison of travel time inversions for marine refraction profiles, *J. Geophys. Res.* **81,** 4061–4070.

Lewis, T. R. and McClain, J. (1977). Converted shear waves as seen by ocean bottom seismometers and surface buoys, *Bull. Seism. Soc. Am.* **67,** 1291–1302.

Lewis, B. T. R. and Snydsman, W. E. (1976). Structure of the crust and upper mantle of the Northern Cocos Plate, 0–12 m.y., *J. Geophys. Res.* (in press).

Maynard, G. L. (1970). Crustal layer of velocity 6.9 to 7.6 km/sec under the deep oceans, *Science* **168,** 120–121.

Orcutt, J. A., Kennett, B. L. N., and Dorman, L. M. (1976). Structure of the East Pacific Rise from an ocean bottom seismometer survey, *Geophys. J.* **45,** 305–320.

Raitt, R. W. (1956). Geophysical measurements, oceanographic instrumentation, Rancho Santa Fe Conference, 21–23 June 1952, *Natl. Acad. Sci. Natl. Res. Council Publ. 309,* Washington, D.C.

Raitt, R. W. (1963). The crustal rocks, in *The Sea,* **3,** 85–102, M. N. Hill, Editor, Interscience, New York.

Raitt, R. W., Shor, G. G., Jr., Francis, T. J. G., and Morris, G. B. (1969). Anisotropy of the Pacific upper mantle, *J. Geophys. Res.* **74,** 3095–3109.

Shor, G. G., Jr., Menard, H. W., and Raitt, R. W. (1971). Structure of the Pacific basin, in *The Sea,* **4,** 3–28, A. E. Maxwell, Editor, Interscience, New York.

Spudich, P. K. P. (1977). Synthetic seismograms from model ocean bottoms, *J. Geophys. Res.* (in press).

Sutton, G. H., Maynard, G. L., and Hussong, D. M. (1971). Widespread occurrence of a high-velocity basal layer in the Pacific found with repetitive sources and sonobuoys, Physical properties of the oceanic crust, Geophys. Monogr. Ser. 14, 193–210, J. Heacock, Editor, Am. Geophys. Union, Washington, D.C.

Woollard, G. P. (1975). The interrelationships of crustal and upper mantle parameter values in the Pacific, Rev. Geophys. Space Physics, **13,** 87–137.

SEISMOLOGICAL LABORATORY
DIVISION OF GEOLOGICAL AND PLANETARY SCIENCES
CALIFORNIA INSTITUTE OF TECHNOLOGY
PASADENA, CALIFORNIA 91125
CONTRIBUTION NO. 2962

Manuscript received August 22, 1977